

# Self-organized adaptive paths in multi-robot manufacturing: reconfigurable and pattern-independent fibre deployment

Catriona Eschke<sup>1,2</sup>, Mary Katherine Heinrich<sup>2</sup>,  
Mostafa Wahby<sup>2</sup>, and Heiko Hamann<sup>2</sup>

<sup>1</sup> Division Metallic Biomaterials, Institute of Materials Research,  
Helmholtz-Zentrum Geesthacht, Germany

<sup>2</sup> Institute of Computer Engineering,  
University of Lübeck, Germany

hamann@iti.uni-luebeck.de

January 2020

## Abstract

Using multi-robot systems for autonomous construction allows for parallelization and scalability. Swarm construction furthermore exploits robot interactions and collaboration, such that the robot swarm collectively constructs artifacts beyond what a single comparable robot could achieve. Here we present an alternative concept of swarm construction that is distinct because it uses continuous building material. Our approach is unique in its use of braiding techniques for construction. We deploy fibres that potentially allow for structures that are not possible with building blocks. To achieve maximal scalability we restrict ourselves to a decentralized approach. The main challenges are the local coordination of the robot teams, self-organized task allocation, and the dynamic reconfiguration of the braiding scheme at runtime. We successfully validate our approach in multi-robot experiments that show both braiding and branching of the braid. In addition, we show options for implementing an open system—that is robots can join and leave the braiding process on the fly.

## 1 Introduction

Self-organized construction [1, 2] is an application scenario of swarm robotics [3] that is particularly rich in its subsumed tasks. Robots may need to collectively decide where to start the construction, heavier building materials may require collective transport [4], and the placement of building material may need a sophisticated degree of coordination and synchronization among the robots [2]. Autonomous construction by multi-robot systems is also relevant because it has high potential for parallelization and even for

synergetic effects by collaboration. Whether high degrees of robustness and scalability as provided by swarm robotics are actually required in an application of autonomous construction should be critically analyzed for a given application scenario. On the one hand, studies in swarm robotics demonstrate that groups of autonomous coordinating devices face significant scalability and robustness limitations when they receive instructions from a centralized detached control system as this resembles a bottleneck and single point of failure. On the other hand, decentralized systems are known to be difficult to develop and handle. Automated guided vehicles (AGVs) are an example of a deployed system that usefully compromises between central components and a decentralized approach [5].

In contrast to common approaches in multi-robot construction using building blocks [2, 6], we use continuous building material that potentially allows for infinitely many shapes and forms. We use mobile robots to braid fibres. Although some self-organization has been implemented in our previous work with line-following robots on predefined tracks [7], swarm robotics approaches to fibre deployment are generally underexplored. Our previous work [7] did not include autonomous initialization, adaptive paths, or reconfigurability during runtime, each of which are important for a swarm approach and are addressed here. Scalability will be a relevant issue in the manufacture even of moderately large braided preforms or soft-body robots, and robustness will be crucial for deployment of on-site construction automation for braided composites or formwork.

Carbon fibre or glass fibre placement in multi-material systems is a common process in industrial manufacturing. Across aerospace, automotive, and other engineering applications, 2D and 3D fibre preforms and composites are produced, for instance, by braiding [8, 9]. Beside composite preforms, braiding has been investigated for soft-body manipulators [10, 11] and locomotion [12, 13]. In on-site construction robotics, there has been a recent surge in research of fibre placement methods, including wound fibre composites [14] and knit concrete formwork [15]. Machinery for braid manufacturing has a long history of development, recently privileging rapid reconfigurability, with newer solutions proposing mobile carrier devices [16] that resemble multi-robot systems. Until now these devices are proposed to follow predetermined paths using centralized control [16], an approach typical of computer-aided manufacturing [17], or to follow lines or other centrally controlled signals [16].

This paper investigates a self-organized approach to the control of mobile braiding robots in a trackless arena, using extended versions of the ‘Thymio II’ [18] robots as a simple testbed hardware platform. An essential difference of our braiding approach to more common swarm construction scenarios using building blocks is that we cannot use stigmergy [19]. The constructed braid is mounted at the ceiling out of the robots’ sight. An advantage is that we could exploit mathematical theories, such as knot and braiding theory [20] that allow abstractions, for example, for methods of de-braiding. From the possible control tasks for self-organized manufacturing and construction [21], here we investigate the tasks of collective group assignment, pattern formation according to the locally sensed environment, and adaptive path finding for material deployment.

This research is related to project *flora robotica* [22, 23, 24] that explores options of growing architectural artifacts by steering the growth of natural plants. Swarm construction is an option to build scaffolds for climbing plants. With autonomous braiding



Figure 1: Thymio II differential drive mobile robot equipped with infrared sensing and communication, extended with Raspberry Pi, RGB color sensor, additional battery, and mechanical attachment of fibre.

systems the braid could be produced around living plants and could exploit the plants' thigmotropism (growth steered by touch) to steer their growth. Using a small and flexible system (e.g., mobile robots) seems a particularly useful option here in non-factory conditions instead of large, inflexible industrial machines.

## 2 Hardware and Experiment Setup

Autonomous mobile carriers for rapidly reconfigurable industrial braiding machines have been developed to a production-ready level [16], equipped for the mobile devices to execute a predetermined path, follow lines, or follow projected cues. We use 'Thymio II' robots as a stand-in hardware platform to investigate our control approach, extending them to have comparable sensing to the industrial version. Although there are well-developed solutions for mechanical treatment of the fibres in industrial setups, here we use only a simplified version of the mechanics, enough to confirm correct pattern formation by our control method.

The Thymio II is a small, simple mobile robot designed for early education scenarios [25], and sometimes extended for university education and research [26], see Fig. 1. Roughly 11 cm square and 5 cm in height, weighing 270 g, it is propelled by differential wheeled drive with two DC motors. Its two wheels are located on either side at the robot's rear, with the front kept level by a low-friction ground-facing protrusion. Its primary sensing capabilities used here are by infrared proximity sensors, with an array of five lateral IR sensors on the front side, two lateral on the rear side, and two ground-facing, along with one infrared remote control receiver. The seven lateral IR sensors can be used for proximity sensing and communication, and the two ground IR sensors can be used for line following or similar tasks. It also has RGB LEDs to display its state to a user. Its normal programming is based on the modular event-based

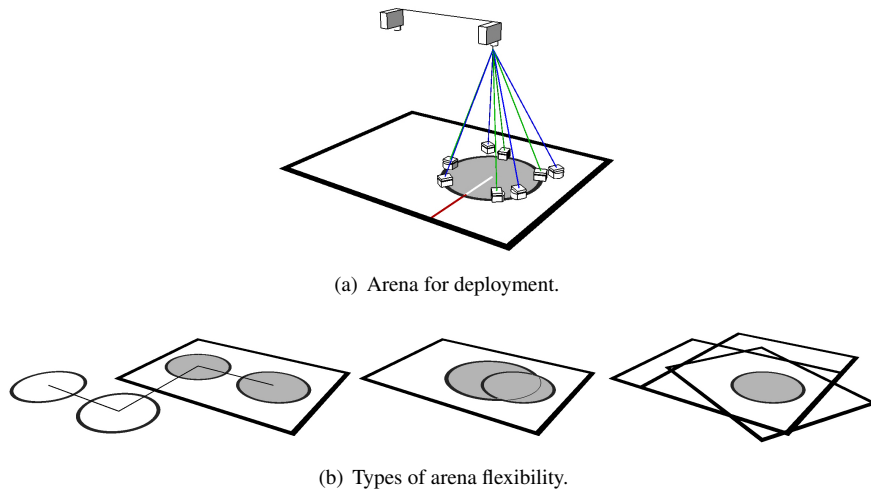
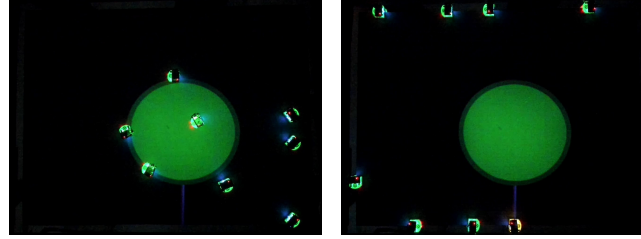


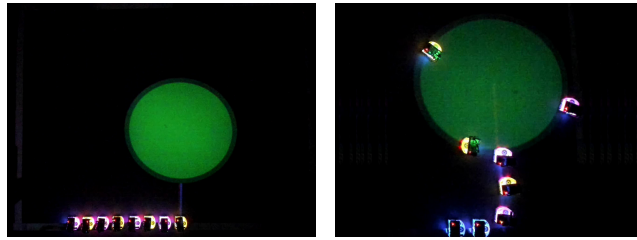
Figure 2: Semi-structured fibre deployment setup. (a) The environment cues are provided by ground-facing video projectors. A lit circle with a partially darker outer border is projected below fixed connections for fibres. The robots identify the border and adaptively navigate around it. Navigation markers (here red) are also projected to link the arena boundary to the circle and interlink neighboring circles, also serving as a seed position during group assignment. (b) The robots follow cues from environmental features in a decentralized way, such that control is not dependant on arena details and they are therefore flexible. (Left) multiple or single projection zones, (center) adjustable size and placement of projection zone, (right) adjustable shape of arena boundary.

architecture ASEBA [27]. The firmware for the Thymio II presents certain limitations for our setup which are resolved via our control algorithms, such as undistinguished sensor identity when receiving IR signals for communication.

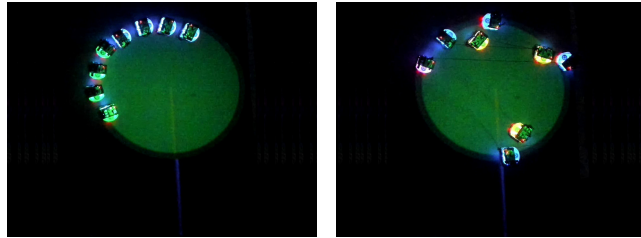
In a multi-robot system context, a group of Thymios can receive synchronous global information by remote control, or asynchronous global information by sensing and interpreting local environmental features. Local robot-robot communication can occur at distances up to approximately 25 cm, when lateral IR sensors from each of the two robots have coincident fields of view, such that the emitter of one aligns with the sensor of the other (with reciprocal alignment for bidirectional communication). IR proximity sensing and robot-robot communication are limited by the positioning of the lateral sensors, with blind spots present at the robots' left and right sides. As the Thymio is a differential drive robot, it will normally approach objects from the front or rear, so this limitation is minor for proximity sensing. However a primary task here is for two self-organizing robots to pass one another while also exchanging IR communication, such that an interaction can fail if one robot initially approaches the other from one of its sides. Thus the mechanisms by which they choose and execute passing must have sufficient tolerance to reliably avoid this type of failure. The robot-robot



(a) Moving forward with obstacle avoidance. (b) Boundary following.



(c) Aggregation and group assignment. (d) Entering deployment zone.



(e) Request fibre attachment. (f) Begin self-organized fibre deployment.

Figure 3: The initialization of  $N = 8$  robots for fibre deployment. (a) The randomly placed robots move straight forward with obstacle avoidance until they find the arena boundary. (b) The robots follow the boundary until they find the navigation marker or a robot-robot communication. The yellow robot here has found the marker and therefore designated itself as the seed for group assignment, assigning itself to group I. (c) When a robot finds robot-robot communication, it stops and assigns itself to the opposite group of the robot it just communicated with. Here, all robots have aggregated behind the navigation marker and the group assignment is complete. (d) After waiting periods associated with arena size, the robots follow the navigation marker until they reach the lit circle, then members of group I turn left and group II turn right. Here group I robots emit yellow, and group II robots emit magenta. (e) Having all aggregated on the lit circle, the robots emit green light to request fibre attachments. (f) The robots start the fibre deployment procedure. Group I robots perform the overtaking behaviors relevant to a defined pattern, whenever they encounter and communicate with group II robots.

messages are 11 bit at 100 ms intervals, with one bit reserved for firmware.

The experiments (see summary video<sup>1</sup>) are conducted in a rectangular arena, see Fig. 2(a), of  $3.0 \times 2.5$  m, with a 7.5 cm reflective boundary that can be reliably detected by the robot's ground sensors. The aspects of control relevant to the arena boundary are not dependant on its shape or type, see Fig. 2(b) (i.e., it could be implemented in an irregular arena bounded by sandbags detectable via proximity sensing). Environmental cues are provided by video projectors mounted 2.5 m above the arena, each able to project a  $1.8 \times 1.1$  m area on the arena floor. In these experiments each activated projector provides a 1.1 m diameter light green circle with a darker green 5 cm wide border, around which the robots self-organize their paths to deploy their fibres into a desired pattern. The control approach is independent of circle dimension—which could change in a larger or smaller arena, see Fig. 2(b)—given a dimension large enough for the robot group size to fit. Although more circles could be used in an extended setup, here we limit to two projectors and two circles, with a 50 cm margin between circles. For each circle, a projected 2 cm wide navigation marker connects it to the arena boundary or a neighboring circle, see red marker in Fig. 2(a). When more than one circle is used, they are projected at distinguishable intensities. The fibres deployed here are 1.2 mm non-elastic synthetic rope in two colors, with fixed top connections 2.5 m above the arena floor and spring bottom connections at each robot. The spring connections consist of 1.2 mm synthetic rope with elastic core. During each experiment, both the robots and the fibres are recorded, via two camera setups.

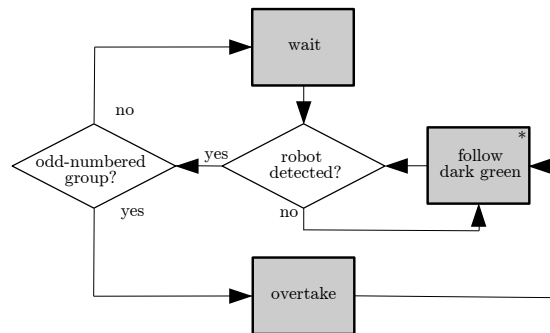


Figure 4: Finite state machine of group I giving an overview of the robot-robot communication and overtake to deploy fibres. The side for passing (left or right) chosen by the group I robot depends on the user-defined pattern and the robot's previous choice. For instance in a  $1 \times 1$  regular biaxial braid, the robot will always pass on the opposite side of its last overtake event.

As the experiments utilize sensing of projected light features, the Thymio hardware is extended to add an RGB color sensor (TCS34725), along with a Raspberry Pi and a 5000 mAh power bank to extend the robot runtime up to four hours. The components are mechanically affixed to the top of the robot, see Fig. 1, and a mechanical attachment for fibres is affixed at the rear, between the sensors. The RGB color sensor provides red,

<sup>1</sup>Video: <https://doi.org/10.5281/zenodo.3357187>.

green, blue, and white light intensities in 16 bit values, includes an infrared filter that prevents interference from the robot-robot communication signals, and is interfaced with the Raspberry Pi via I<sup>2</sup>C bus with 154 ms integration time. The Raspberry Pi is connected to the robot via D-Bus interface and USB port. In addition to interfacing with the sensor, adding a single-board computer allows the control algorithms to be implemented in Python, connected to the robot's firmware via an ASEBA middleware.

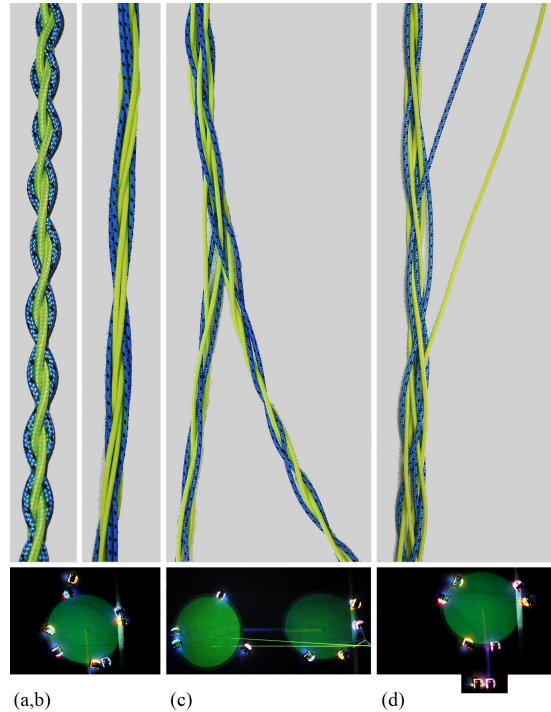


Figure 5: Different types of fibre patterns deployed by consistent robot-robot interactions, triggered into distinct execution by limited global signals or cues. (a)  $1 \times 1$  regular biaxial braid of 4 fibres, (b)  $2 \times 2$  regular biaxial braid of 8 fibres, (c) 8 fibre biaxial braid branching into two 4 fibre braids, (d) 8 fibre biaxial braid where two fibres leave, modifying the pattern on the fly (braid results from robots leaving or joining mid-way look similarly). The respective setups for these results are shown beneath them. (a,b) The regular setup of all robots navigating a single-circle environment. (c) Robots navigating a two-circle environment, allowing branching. (d) Six robots navigating the circle, while two additional robots wait below, to join on the fly when signaled.

## 3 Control Algorithms and Results

### 3.1 Seed aggregation and group assignment

Task allocation as it is commonly implemented in swarm robotics [28] is not suitable here because these are typically based on probabilistic control techniques steering populations of robots but here we need a precise deterministic allocation for a rather small team of robots. Using a finite state machine approach with four sequential states prior to fibre attachment, the robots move around with obstacle avoidance, follow the boundary to aggregate at a seed position indicated by a navigation marker, and finally assign themselves into groups using local communication. This control algorithm is tested in six experiment repetitions. All repetitions are fully successful—see frames of one repetition in Fig. 3—with no failures in detection, communication, or decision.

At each initialization the robots are distributed roughly equally across the arena, at variable arbitrary start positions, see Fig. 3(a). After receiving a starting signal by remote control they move forward searching for the arena boundary, except for when they detect an obstacle by IR proximity sensing where they turn left for a random duration between 1 and 6 s. Once the boundary is found, the robots perform a counter-clockwise line following until they find the navigation marker or complete a successful robot-robot IR signal with the robot queue, see Figure 3(b). If a robot finds the navigation marker it stops and seeds group assignment. It assigns itself to group I, then waits for  $t = 0.45b$ , where  $b$  is the arena perimeter in meters, guaranteeing enough time for all robots to stack in the queue without any global broadcasting. When a robot joins the queue by robot-robot IR signal, it receives the group assignment of the robot in front of it, and then assigns itself the opposite group. The robots subsequently assign themselves alternating numbers, until all are divided into equal sized groups. For most deployment experiments here there are only two groups—group I and group II, see Fig. 3(c)—but sometimes will be more groups, such as four groups for branching. Generally, there are two robot groups for every circle projected in the arena.

After successful group assignment, the robots follow the navigation marker until they reach the lit circle, see Fig. 3(d) To begin the deployment process, the robots must organize themselves into starting positions appropriate to the task. They need to distribute themselves evenly around the sensed environment feature (i.e., the lit green circle) in an alternating pattern, with the members of the two groups facing opposing radial directions. Therefore, once they reach the circle, group I members turn left and group II members turn right. They follow the dark green color, until the two groups meet. To ensure that the braiding process does not start before all robots arrive, they each wait for 40 s, then group II members turn  $180^\circ$  and follow the circle until they meet the last member of group I. Now, they turn around again, and all robots emit green to request fibre attachment, see Fig. 3(e). This process of moving into position after group assignment, while here accomplished by robots physically relocating, can also be executed by distributed information transfer with adjacent neighbors. After the user confirms fibre attachments, as long as a robot does not see itself being blocked by another robot, it waits 60 s then starts the fibre deployment procedure, see Fig. 3(f).

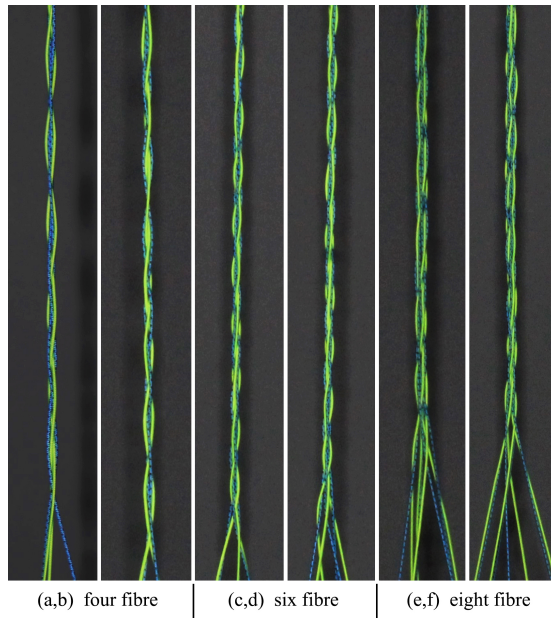


Figure 6: Experiment repetitions give self-consistent results, and the distributed multi-robot deployment strategy is shown to scale without modification to control, and without robots knowing information about swarm size. Scaling is implemented simply by adding more robots to the arena at initialization. (a,b) Two consecutive runs of a 4 fibre biaxial braid, (c,d) two runs of 6 fibre, and (e,f) two runs of 8 fibre.

### 3.2 Pattern-independent adaptive paths

By using a generic trackless arena for fibre deployment, the robots can perform any biaxial  $x \times y$  braid pattern, i.e., two robot groups move in opposite directions around the circle and pass each other according to the pattern (see finite state machine in Fig. 4). In a regular  $1 \times 1$  braid pattern (i.e., one fibre from one group crosses one fibre from the other group), see Figs. 5 and 6, the odd-numbered robot groups overtake the members of even-numbered groups in an alternating left-right who in turn wait to be passed. In a  $2 \times 2$  braid pattern (i.e., two fibres from one group cross two fibres from the other group), see Fig. 5, the behavior will differ in that two consecutive odd-numbered group robots will pass on the same side in two consecutive passing events before switching. The passing behaviour is controlled locally by robot-robot IR signals, light intensity and proximity sensing as well as the robots keeping track of the last passing sides. This way, the overall number of braiding robots is not relevant. When the robots initialize a  $1 \times 1$  braid, they first pass on side opposite the robot in front of them. As the robots are distributing themselves roughly equally at this stage, they need to choose opposite passing sides in order to self-synchronize, such that during the deployment process they will each be passing on self-similar sides roughly concurrently. This is an important behavior for braided patterns built by self-organization, as the individual fibre trades in one braid row need to match.

The current desired braiding pattern is set according to a global parameter updatable by remote control. Also possible to trigger by remote control is certain robots leaving on the fly. Because of the distributed approach the remaining robots do not need to receive any global notice but react to changes in local perception and reorganize themselves to retain a correct braid pattern. Robots can also be added on the fly in this manner, again without giving notice to the other robots. For branching of a braid, two environment circles are required in the setup. The robots will self-assign into four groups in this case. While the braid is merged, all four groups will run on one circle, and groups I and III will act as one, while groups II and IV act as one. When branching is triggered by remote control, groups III and IV move to the neighboring circle and proceed with their normal behavior there instead, thus creating a branching event in the deployed fibres. The following experiments are successfully conducted with three repetitions each: 4 fibre regular, 6 fibre regular, 8 fibre regular, 8 fibre  $2 \times 2$  pattern, branching 8 fibre, 2 robots leaving, and 2 robots joining (see dataset of recorded experiments<sup>2</sup>).

## 4 Discussion and Conclusions

Here we sometimes reach the limits of hardware reliability in the Thymio II robots, as for instance an IR sensor will occasionally malfunction or a wheel will not turn when indicated. As here we use only a stand-in hardware and look primarily at high-level control, we tolerate minor hardware disturbance in the experiments. When hardware functions were interrupted, we used manual intervention to compensate (as seen in the

---

<sup>2</sup>Robot view: <https://doi.org/10.5281/zenodo.3360845>. Fibre view: <https://doi.org/10.5281/zenodo.3360809>.

experiment videos). Hardware failures each lasted a few seconds, occurring at  $\leq 2\%$  of robot-robot interactions, and during  $\leq 0.5\%$  of experiment time.

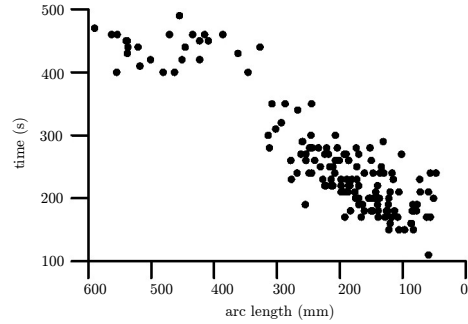
Image sampling is used to extract information about individual robot-robot events from the recorded videos. Videos are sampled every 1 s, at 1/10th resolution. From this we analyze the relationship between density and performance, in relation to swarm scaling [3]. As seen in Fig. 7(a), duration of passing events unsurprisingly decreases as the starting distance decreases, with a more extreme step occurring at around 350 mm. Less intuitively, as seen in Fig. 7(b), speed per passing event also generally decreases as the starting distance decreases. Driving around the environment circle unobstructed is faster than the execution of passing. The decline in speed per passing event becomes substantially steeper below arc lengths of roughly 250 mm, as at these distances, the robots are located too densely and begin to cause interference for their neighbors, as for instance a passing robot may collide with its subsequent partner before it has finished passing its current partner, causing a traffic jam as all robots need to adjust backwards and forwards until sufficient space has been cleared to resolve the interference. Considering the better performance in Fig. 7(a) at lengths under 200–250 mm, and the better performance in Fig. 7(b) at lengths over 250–300 mm, we consider that the performance of this multi-robot system peaks approximately at an arc length of 200–300 mm. The size of the arena and environment features can be optimized according to this understanding of performance, such that the density of robots keeps robot-robot distances roughly within this ideal range, at the start of a new passing event.

## References

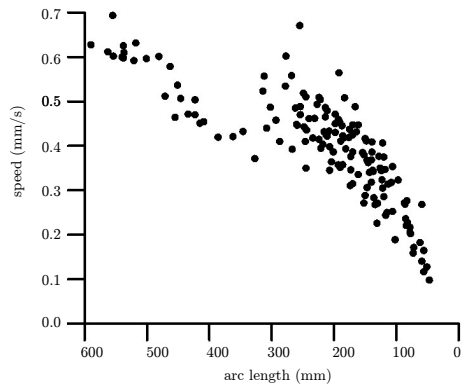
- [1] H. Hamann, S. von Mammen, and I. Mauser, “Special issue on self-organised construction,” *Swarm Intelligence*, vol. 12, no. 2, pp. 97–99, Jun 2018. [Online]. Available: <https://doi.org/10.1007/s11721-017-0154-5>
- [2] J. Werfel, K. Petersen, and R. Nagpal, “Designing collective behavior in a termite-inspired robot construction team,” *Science*, vol. 343, no. 6172, pp. 754–758, 2014. [Online]. Available: <http://science.sciencemag.org/content/343/6172/754>
- [3] H. Hamann, *Swarm Robotics: A Formal Approach*. Springer, 2018.
- [4] S. Wilson, T. P. Pavlic, G. P. Kumar, A. Buffin, S. C. Pratt, and S. Berman, “Design of ant-inspired stochastic control policies for collective transport by robotic swarms,” *Swarm Intelligence*, vol. 8, no. 4, pp. 303–327, 2014.
- [5] P. R. Wurman, R. D’Andrea, and M. Mountz, “Coordinating hundreds of cooperative, autonomous vehicles in warehouses,” *AI magazine*, vol. 29, no. 1, p. 9, 2008.
- [6] M. Allwright, N. Bhalla, H. El-faham, A. Antoun, C. Pinciroli, and M. Dorigo, “SRoCS: Leveraging stigmergy on a multi-robot construction platform for unknown environments,” in *Int. Conf. on Swarm Intelligence*. Springer, Cham, 2014, pp. 158–169.

- [7] M. K. Heinrich, M. Wahby, M. D. Soorati, D. N. Hofstadler, P. Zahadat, P. Ayres, K. Støy, and H. Hamann, “Self-organized construction with continuous building material: Higher flexibility based on braided structures,” in *2016 IEEE 1st International Workshops on Foundations and Applications of Self\* Systems (FAS\*W)*, Sept 2016, pp. 154–159.
- [8] K. Bilisik, “Three-dimensional braiding for composites: a review,” *Textile Research Journal*, vol. 83, no. 13, pp. 1414–1436, 2013.
- [9] Z. Quan, A. Wu, M. Keefe, X. Qin, J. Yu, J. Suhr, J.-H. Byun, B.-S. Kim, and T.-W. Chou, “Additive manufacturing of multi-directional preforms for composites: opportunities and challenges,” *Materials Today*, vol. 18, no. 9, pp. 503–512, 2015.
- [10] M. Cianchetti, M. Calisti, L. Margheri, M. Kuba, and C. Laschi, “Bioinspired locomotion and grasping in water: the soft eight-arm octopus robot,” *Bioinspiration & biomimetics*, vol. 10, no. 3, p. 035003, 2015.
- [11] T. Hassan, M. Cianchetti, B. Mazzolai, C. Laschi, and P. Dario, “Active-braid, a bioinspired continuum manipulator,” *IEEE Robotics and Automation Letters*, vol. 2, no. 4, pp. 2104–2110, 2017.
- [12] S. Seok, C. D. Onal, R. Wood, D. Rus, and S. Kim, “Peristaltic locomotion with antagonistic actuators in soft robotics,” in *2010 IEEE International Conference on Robotics and Automation*, May 2010, pp. 1228–1233.
- [13] T. Manwell, T. Vítek, T. Ranzani, A. Menciassi, K. Althoefer, and H. Liu, “Elastic mesh braided worm robot for locomotive endoscopy,” in *Proc. 36th Annu. Int. Conf. IEEE Eng. Med. Biol. Soc.*, 2014, pp. 848–851.
- [14] R. La Magna, F. Waimer, and J. Knippers, “Coreless winding and assembled core—novel fabrication approaches for frp based components in building construction,” *Construction and Building Materials*, vol. 127, pp. 1009–1016, 2016.
- [15] M. Popescu, L. Reiter, A. Liew, T. Van Mele, R. Flatt, and P. Block, “Building in concrete with a knitted stay-in-place formwork: Prototype of a concrete shell bridge,” *Structures*, vol. 14, pp. 322–332, June 2018.
- [16] A. A. Head and V. M. Ivers, “Rapidly configurable braiding machine,” Dec. 29 2015, uS Patent 9,222,205.
- [17] D. M. Dilts, N. P. Boyd, and H. Whorms, “The evolution of control architectures for automated manufacturing systems,” *Journal of manufacturing systems*, vol. 10, no. 1, pp. 79–93, 1991.
- [18] F. Mondada, M. Bonani, F. Riedo, M. Briod, L. Pereyre, P. Rétornaz, and S. Magnenat, “The Thymio open-source hardware robot,” *IEEE Robotics & Automation Magazine*, vol. 1070, no. 9932/17, p. 2, 2017.
- [19] E. Bonabeau, Ed., *Special issue on Stigmergy*, ser. Artificial Life Journal. MIT Press, 1999, vol. 5.

- [20] W. Menasco and M. Thistlethwaite, Eds., *Handbook of Knot Theory*. Elsevier, 2005.
- [21] V. Gerling and S. Von Mammen, “Robotics for self-organised construction,” in *Foundations and Applications of Self\* Systems, IEEE International Workshops on*. IEEE, 2016, pp. 162–167.
- [22] H. Hamann, M. Wahby, T. Schmickl, P. Zahadat, D. Hofstadler, K. Støy, S. Risi, A. Faina, F. Veenstra, S. Kernbach, I. Kuksin, O. Kernbach, P. Ayres, and P. Wojtaszek, “*flora robotica* – mixed societies of symbiotic robot-plant bio-hybrids,” in *Proc. of IEEE Symposium on Computational Intelligence (IEEE SSCI 2015)*. IEEE, 2015, pp. 1102–1109. [Online]. Available: <http://dx.doi.org/10.1109/SSCI.2015.158>
- [23] H. Hamann, M. Divband Soorati, M. K. Heinrich, D. N. Hofstadler, I. Kuksin, F. Veenstra, M. Wahby, S. A. Nielsen, S. Risi, T. Skrzypczak, P. Zahadat, P. Wojtaszek, K. Støy, T. Schmickl, S. Kernbach, and P. Ayres, “*flora robotica* - An architectural system combining living natural plants and distributed robots,” *arXiv preprint arXiv:1709.04291*, 2017.
- [24] *flora robotica*, “project website,” 2019, <http://www.florarobotica.eu>.
- [25] F. Riedo, M. Chevalier, S. Magnenat, and F. Mondada, “Thymio II, a robot that grows wiser with children,” in *IEEE Workshop on Advanced Robotics and its Social Impacts (ARSO)*. IEEE, 2013, pp. 187–193.
- [26] J. Guzzi, A. Giusti, G. A. Di Caro, and L. M. Gambardella, “Mighty thymio for university-level educational robotics,” 2018.
- [27] S. Magnenat, P. Rétornaz, M. Bonani, V. Longchamp, and F. Mondada, “ASEBA: A modular architecture for event-based control of complex robots,” *Mechatronics, IEEE/ASME Transactions on*, vol. 16, no. 2, pp. 321–329, 2011.
- [28] M. Brambilla, E. Ferrante, M. Birattari, and M. Dorigo, “Swarm robotics: a review from the swarm engineering perspective,” *Swarm Intelligence*, vol. 7, no. 1, pp. 1–41, 2013.



(a) Duration of robot-robot interactions.



(b) Overall speed of robot-robot interactions.

Figure 7: The first 50 robot-robot interactions for each of the three regular pattern experiments demonstrating scalability (4 fibres, 6 fibres, 8 fibres), as identified by image sampling of the experiment video recordings. (In total, the first 150 interactions.) Duration and speed of the individual robot-robot interactions for passing, according to the starting distance between their center points, as measured along the circumference of the circle environment feature in radial mm along the arc. A robot-robot interaction is considered complete if the passing robot has returned to the environment circle, and has also overtaken the other respective robot by a margin of 20 mm. A new robot-robot interaction is considered to begin once the passing robot's previous interaction has terminated. (a) Duration of a full passing event, (b) overall speed during a full passing event.